THE AMERICAN MINERALOGIST, VOL. 46, SEPTEMBER-OCTOBER, 1961

POLYMORPHISM OF ABO_3 TYPE RARE EARTH BORATES*

ERNEST M. LEVIN, ROBERT S. ROTH AND JERRY B. MARTIN,†
National Bureau of Standards, Washington, D. C.

ABSTRACT

Polymorphic relationships as a function of temperature and ionic radius were investigated for thirteen ABO_3-type borates, including all of the normally trivalent rare earth ions as well as La^{+3}, Y^{+3}, In^{+3}, and Mn^{+3}. The melting points of the compounds varied irregularly from 1660° C. for $LaBO_3$ to 1540° C. for $EuBO_3$. In general, the borate compounds exhibited the same structure types as the three forms of $CaCO_3$, *i.e.*, aragonite, vaterite, and calcite. Compounds of the larger ions, $LaBO_3$ and $NdBO_3$, showed the aragonite-type structure at low temperature. These compounds were found to have a reversible transformation at 1488° C. and 1090° C., respectively. The high-temperature forms were different from each other, and both exhibited low symmetry. The following borates showed a stable vaterite-type phase: $SmBO_3$, $EuBO_3$, $GdBO_3$, $DyBO_3$, YBO_3, $HoBO_3$, $ErBO_3$, $TmBO_3$, $YbBO_3$, and $LuBO_3$. Above 1285° C., $SmBO_3$ inverted to the high-$NdBO_3$ type polymorph. Below 1310° C., $LuBO_3$ formed the calcite-type structure. No polymorphism was observed in the eight intermediate borates. Indium borate showed only the calcite-type structure. A discussion of the factors affecting polymorphism, such as radius ratio, density, and pressure, in addition to interpretation of infrared and structure data may explain why the vaterite-type structure is more stable in the borates than in the carbonates. Unit cell dimensions are listed for indexed *x*-ray diffraction powder patterns, together with limited optical data. Published *x*-ray powder data for vaterite are compared.

INTRODUCTION

The increasing availability of purified rare earth oxides has served as an impetus to the study of systems containing these oxides. The lanthanide series is significant from a crystal chemical standpoint because it consists of a large, nearly homologous chemical group within the periodic table, in which ionic radius varies from 1.15 Å for lanthanum to 0.85 Å for lutecium. Thus the effect of ionic radius can be studied on such properties as compound formation, solid solution and immiscibility.

Compounds equimolar in R_2O_3 and B_2O_3 are of the ABO_3 type. The classic study on the "Isomorphism of Borates and Carbonates" was made by Goldschmidt and Hauptmann (1931–32). They studied the lanthanum, indium, scandium, and yttrium borates. Lanthanum borate was found to have the $CaCO_3$-aragonite type structure, whereas the other borates were found to be of the $CaCO_3$-calcite type structure, with YBO_3 possibly possessing a $CaCO_3$-vaterite polymorph.

In a major study of the double oxides of trivalent elements, Keith and Roy (1954) included a few experiments on equimolar mixtures of

* Presented at 17th Annual Pittsburgh Diffraction Conference, Nov. 11, 12 and 13, 1959, Mellon Institute, Pittsburgh, Pa.

† Guest worker, summer 1959, from Vanderbilt University, Tenn.

lanthanum, yttrium, indium, and chromium oxides with boric oxide. They noted a high form of $LaBO_3$ but no calcite polymorph of YBO_3.

None of the compounds mentioned are true rare earth borates. Thus it is evident that phase studies in the rare earth borate systems offer a relatively unexplored field. Such studies, along with crystal chemical implications might prove helpful, moreover, in interpreting the complex polymorphic relationships among the carbonates of divalent cations.

The primary objective of this study, therefore, was to investigate the equimolar compositions of boric oxide and the normally trivalent rare earth oxides. In addition, because of ionic radii considerations, Y_2O_3, In_2O_3, and Mn_2O_3 were included. The information on ABO_3 polymorphs was to serve also as a starting point for the more complete study of selected rare earth oxide-boric oxide systems (Levin, *et al.*, 1961).

Materials and Methods

Starting Materials

Starting materials for the preparation of mixtures consisted of reagent grade boric acid powder and thirteen high-purity oxides obtained either commercially or from the Bureau of Mines. The results of general qualitative spectrochemical analyses of these oxides are given elsewhere (Schneider and Roth, 1960; Schneider, 1960). The purity of the oxides, except for Y_2O_3 (99.7%), was better than 99.9%.

Preparation of Mixtures

Calculated amounts of boric acid and of the respective oxides sufficient to yield 1, 2, or 3- g batches of the 1:1 composition were weighed into plastic containers and thoroughly blended for $\frac{1}{2}$ hr. with a high-speed mechanical mixer. In the preparation of mixtures, 0.3 (wt. %) excess of the calculated amount of boric acid (equivalent to about 0.2% excess B_2O_3) was added to compensate for possible volatilization during heating. Mixtures were pressed at approximately 20,000 psi into discs, $\frac{5}{8}$ in. in diameter; fired slowly to 600° or 700° C., in covered platinum crucibles; and ground in an agate mortar. The process of pressing, heating, and grinding was repeated twice at successively higher temperature intervals, up to a maximum of 900° C. Subsequent "quenching" experiments were done in sealed platinum tubes.

The following representative samples were analyzed by the Chemistry Division of the National Bureau of Standards: $LaBO_3$, $NdBO_3$, $GdBO_3$, $TmBO_3$, and $InBO_3$. Analyses were made on approximately 0.2 g samples, for B_2O_3 only. The results indicated that the samples were deficient in B_2O_3, about 0.5 mol % for $LaBO_3$, $NdBO_3$, and $GdBO_3$; about 0.75 mol % for $TmBO_3$; and about 2 mol % for $InBO_3$. The intermediate com-

pounds would be expected to show similar deviations. As will be noted later, *x*-ray examination also indicated that some of the heated samples deviated slightly from the equimolar ratio of B_2O_3 to rare-earth oxide.

Apparatus and Method

The temperatures of polymorphic inversions were determined by the well-established quenching technique. Quenched samples were examined mainly by *x*-ray diffraction powder techniques (Ni-filtered Cu radiation) using a high angle Geiger-counter diffractometer. Where possible, optical data were obtained with the aid of the polarizing microscope. Temperatures were measured with a calibrated platinum versus platinum-rhodium (10%) thermocouple and are given on the International Temperature Scale of 1948. Unless otherwise stated temperature values may be considered accurate to within $\pm 10°$ C. up to about 1300° C., and to within $\pm 15°$ C. at higher temperatures.

Melting points of the compounds were determined in air in a specially designed, inductively heated iridium crucible (Schneider, 1961). Small fragments of material, approximately 1 to 2 mm. in length, were placed in the covered iridium crucible and quickly cooled from various temperatures, by shutting off the power. Temperatures were measured with a calibrated optical pyrometer which was sighted through a hole in the center of the crucible cover. Approximate blackbody conditions prevailed, and the equipment was calibrated against the melting points of Au (1063° C.), Pt (1769° C.) and Rh (1960° C.). Reproducibility of temperature measurements by this method is within $\pm 10°$ C., accuracy better than $\pm 20°$ C.

Results and Discussion

General Relationships

Table 1 lists the significant quenching experiments and includes the temperatures and periods of heat treatments, demonstrations of reversibility, and phases identified by *x*-ray analysis. The complete data are summarized in Fig. 1, in which the cations are listed along the abscissa, as a function of ionic radius. The dashed lines between adjacent compounds are postulated phase boundaries. The boundaries would probably not be applicable for mixtures of other than adjacent compounds. Melting points of the compounds, as determined with the induction apparatus, are shown by solid squares. Numerical values are given alongside the appropriate cation designations.

The most striking result of this study is that the ABO_3 rare-earth borates possess the same types of structures as calcium carbonate, namely, aragonite, vaterite, and calcite. Of particular interest is the

existence of the vaterite type as a stable phase for ten of the borates. In the $CaCO_3$ system vaterite is apparently only a metastable phase. It may be noted that no one borate compound shows all three polymorphs, as in the case of $CaCO_3$. In fact, only $LuBO_3$ shows two of the polymorphs, *i.e.*, calcite and vaterite. Lanthanum and neodymium borates both show unidentified high-temperature forms.

With decreasing ionic radius, the melting points of the ABO_3 type rare-earth borates decrease from a maximum of $1660 \pm 20°$ C. for $LaBO_3$

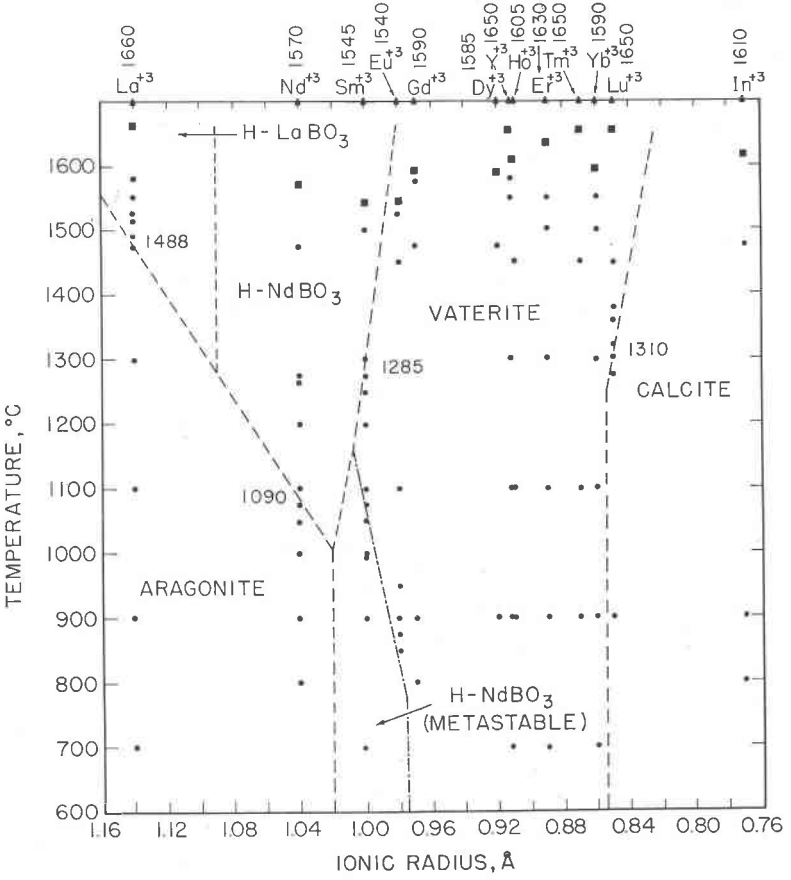

FIG. 1. Stability relationships of the ABO_3-type borates as a function of temperature and ionic radius of the large cation. Temperatures of reversible transitions listed within the diagrams. Dots represent subsolidus experiments. Squares represent liquidus values, given along the top of the figure. Dashed lines indicate boundaries between adjacent ABO_3 compounds. Dash-dot line indicates limit of formation of the metastable high-temperature form in the vaterite field.

to a minimum of 1540 ± 20° C. for $EuBO_3$. The melting points, except for $YbBO_3$ (M. Pt. 1590 ± 20° C.), then increase to a maximum of 1650 ± 20° C. for $LuBO_3$. The non rare-earth borates, YBO_3 and $InBO_3$, melt at 1650 ± 20° C. and 1610 ± 30° C. respectively.

The limitation in accuracy of the melting point determinations is due not so much to the accuracy of temperature measurements but rather to the small variation from compound composition, as revealed by chemical analysis and by some of the *x*-ray diffraction powder patterns. Patterns of the compounds containing the larger ions of La, Nd, Sm, Eu, Gd, and Dy showed a single phase. Vaterite patterns of the borates of Y, Ho, Er, Tm, and Yb showed a few weak extraneous peaks in the 26 to 30° 2θ region. These additional peaks were tentatively ascribed to the compounds of molar ratio 3 R_2O_3 to 1 B_2O_3, as a result of experiments on mixtures of Tm_2O_3 and B_2O_3 (footnote d, Table 1). A compound of the same molar ratio has been found in the La_2O_3-B_2O_3 system (Levin, *et al.*, 1960). Patterns of the compounds of the two smallest ions, Lu and In, showed free Lu_2O_3 and In_2O_3, respectively, indicating that no intermediate compounds form between 1:1 and R_2O_3.

Aragonite Type ABO_3 Rare-Earth Borates

Table 2 gives the indexed *x*-ray diffraction data for $LaBO_3$ and $NdBO_3$, aragonite-type structures, compared with that for $CaCO_3$. The aragonite type structure is orthorhombic, space group Pnam (No. 62), Z = 4. The unit cell dimensions determined for $LaBO_3$ are $a = 5.104$ Å, $b = 8.252$ Å, $c = 5.872$ Å; for $NdBO_3$, $a = 5.037$ Å, $b = 8.076$ Å, $c = 5.729$ Å. The powder patterns for the three compounds are shown diagrammatically in Figure 2. For $CaCO_3$ the *a* axis and the *b* axis are smaller than for $NdBO_3$ and $LaBO_3$, whereas the *c* axis is slightly larger than for $NdBO_3$. These relationships are indicated by the position of the 200, 041, and 002 reflections. The data of Goldschmidt and Hauptmann (1931–32) (Table 2) are in reasonable agreement with the present work. The neodymium ion is the smallest rare earth ion to form an aragonite-type borate. The borates of trivalent praesodymium and cerium, with ionic radii intermediate between lanthanum and neodymium, would be expected also to show an aragonite form.

High-Temperature Polymorphs

Lanthanum borate inverted at 1488 ± 5° C. to a high-temperature form of low symmetry. As may be seen from Table 3, this form has the same powder pattern as that obtained by Keith and Roy (1954) below 1560° C.; however, the optical properties discussed elsewhere (Levin, *et al.*, 1961) do not agree.

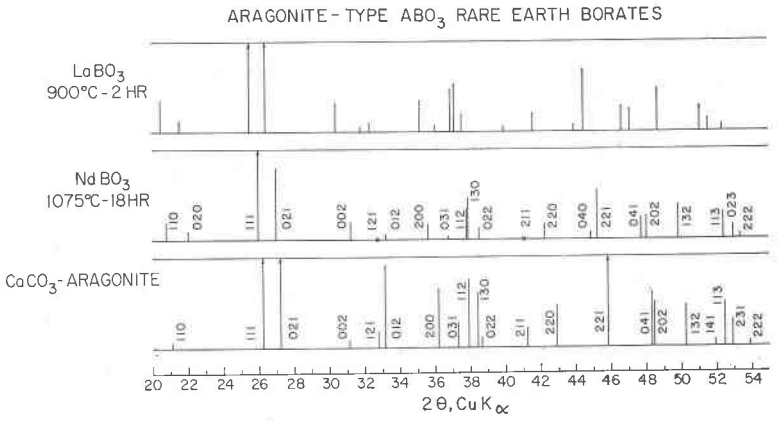

FIG. 2. Diagramatic *x*-ray diffraction patterns of the aragonite-type ABO_3 borates compared with $CaCO_3$. $CaCO_3$-aragonite after Swanson, Fuyat and Ugrinic (1954).

Neodymium, samarium, and europium borates yielded high temperature forms similar to each other but different from lanthanum borate (Fig. 3). The *x*-ray powder diffraction data for the high-$NdBO_3$ type polymorph are given in Table 4. Neodymium borate transformed reversibly at 1090° C. to the high form (Fig. 1). Samarium borate showed a reversible transformation above 1285° C. to the high form; below 1050° C. the high form occurred metastably. The high-temperature form of $EuBO_3$ was never obtained as a single major phase but occurred metas-

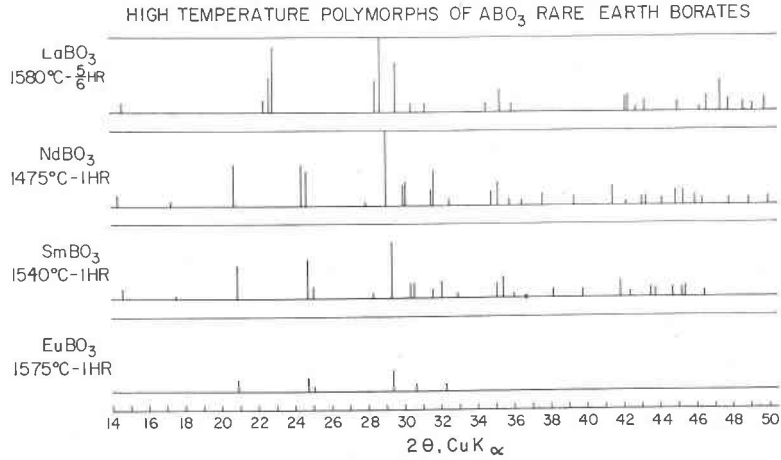

FIG. 3. Diagramatic *x*-ray diffraction patterns of the unindexed high-temperature polymorphs of ABO_3 borates. $LaBO_3$ differs from $NdBO_3$, $SmBO_3$, and $EuBO_3$.

TABLE 1. PHASES IDENTIFIED IN THE ABO_3 TYPE RARE EARTH BORATES

Compound	Heat Treatment[a] Temp., ° C.	Time, hrs.	X-Ray[b]	Notes
$LaBO_3$	700	1.5	Aragonite	
	1475	1	Aragonite	Pattern indexed
	1525/1475[c]	0.67/1	Arag. (l)+H-Form(s)	Shows reversibility
	1490	1	H-Form	
	1580	0.83	H-Form	Pattern measured
$NdBO_3$	800	2	Aragonite	
	1075	18	Aragonite	Pattern indexed
	1100/1075[c]	2/18	Aragonite	Shows reversibility
	1100	2	H-Form	
	1475	1	H-Form	Pattern measured
$SmBO_3$	700	1.5	H-Form	
	1000	65	H-Form	
	1100/1000[c]	15/92	Vaterite	Vaterite not reversible to H-Form at lower temp.
	1050	68.5	H-Form	
	1050	133	H-Form	
	1100/1050[c]	16/64	Vaterite	
	993/1080[c]	16/16	Vaterite (l)+H-Form (m)	
	1100	64	Vaterite	
	1500/1240[c]	1.17/5.5	Vaterite	Shows reversibility at higher temp.
	1275	1	Vaterite	
	1300	2	H-Form	
	1200/1309[c]	24/21	H-Form	
	1540	1	H-Form	Measured pattern
$EuBO_3$	900/850[c]	2/15.5	Vaterite (m)+H-Form (s)	
	900/850/875[c]	2/15.5/15	Vaterite	Metastable H-Form disappeared.
	900	2	Vaterite (l)+H-Form (m)	
	950	15.5	Vaterite	
	1450	1	Vaterite	Pattern indexed
	1540	0.5	Vaterite	
	1575	1	Vaterite (l)+H-Form (m)	Sample melted
$GdBO_3$	800	2	Vaterite	
	1475	1	Vaterite	Pattern indexed
	1575	1	Vaterite	
$DyBO_3$	800	2	Vaterite	
	1475	0.75	Vaterite	Pattern indexed
YBO_3	700	1	Vaterite (l)+Y_2O_3 (s)	
	900	2	Vaterite	
	1100	15	Vaterite	
	1300	2	Vaterite (l)+$3Y_2O_3 \cdot B_2O_3$[d]? (tr).	
	1580	1	Vaterite (l)+$3Y_2O_3 \cdot B_2O_3$[d]? (tr).	Pattern indexed

[a] All heat treatments above 900° C. done in sealed platinum tubes.

[b] When more than one phase is present, the relative amounts are given as: l=large, m=moderate, s=small, tr=trace.

[c] Indicates successive heat treatments of the same sample.

[d] Compositions 95 mol% TM_2O_3, 5 mol% B_2O_3 and 66.67 mol% Tm_2O_3, 33.33 mol% B_2O_3 heated at 1490° C. for 1 hr. showed major peaks corresponding to this unknown phase, indicating a compound intermediate between the pure oxide and the 2 to 1 ratio with B_2O_3.

TABLE 1—(*continued*)

Compound	Heat Treatment[a] Temp. ° C.	Time, hrs.	*X*-Ray[b]	Notes
$HoBO_3$	900	2	Vaterite	
	1100	10	Vaterite	
	1450	1	Vaterite+$3Ho_2O_3 \cdot B_2O_3$[d]? (tr).	Pattern iddexed
$ErBO_3$	700	1.5	Vaterite (l)+Er_2O_3 (m)	
	900	2	Vaterite	
	1100	15	Vaterite (l)+$3Er_2O_3 \cdot B_2O_3$[d]? (s)	
	1300	23	Vaterite (l)+$3Er_2O_3 \cdot B_2O_3$[d]? (s)	Heated in open Pt tube
	1550	1	Vaterite (l)+$3Er_2O_3 \cdot B_2O_3$[d]? (s)	Pattern indexed
$TmBO_3$	900	2	Vaterite	
	1100	19	Vaterite (l)+$3Tm_2O_3 \cdot B_2O_3$[d]? (s)	
	1450	1	Vaterite (l)+$3Tm_2O_3 \cdot B_2O_3$[d]? (m)	
$YbBO_3$	700	1.5	Vaterite (l)+Yb_2O_3 (l)	
	1100	15	Vaterite (l)+Yb_2O_3 (s)	
	1300	2	Vaterite (l)+$3Yb_2O_3 \cdot B_2O_3$[d]? (tr)	
	1550	1	Vaterite (l)+$3Yb_2O_3 \cdot B_2O_3$[d]? (tr)	Pattern indexed
$LuBO_3$	900	2	Calcite (l)+Lu_2O_3 (m)	
	1100	19	Calcite (l)+Lu_2O_3 (m)	
	1275	1	Calcite (l)+Lu_2O_3 (m)	
	1450/1275[c]	1/1	Vaterite (l)+Calcite (l)+Lu_2O_3 (m)	Calcite to vaterite inversion reversible
	1297	17	Calcite (l)+Lu_2O_3 (m)	Pattern indexed
	1320	1	Vaterite (l)+Calcite (m)+Lu_2O_3 (s)	
	1450	1	Vaterite (l)+Lu_2O_3 (m)	Pattern indexed
$InBO_3$	800	2	Calcite (l)+In_2O_3 (l)	
	900	18	Calcite (l)+In_2O_3 (m)	
	1475	0.75	Calcite (l)+In_2O_3 (m)	Pattern indexed
$Mn_2O_3:B_2O_3$	600	1.25	MnO_2 (l)+Mn_2O_3 (m)	
	800	5	Mn_2O_3	
	900	16	Unidentified	Not a $CaCO_3$ type structure

tably in minor amounts in samples quenched from above the liquidus or as prepared below 900° C.

Vaterite-Type ABO_3 Borates

A brief review of the literature concerning vaterite is given in the appendix.

Table 5 gives the *x*-ray diffraction data for the ten borates found in this study to possess the vaterite-type structure. The diagrammatic comparison of the diffraction patterns (Fig. 4) shows that they agree with the $CaCO_3$-vaterite pattern of DeKeyser and Degueldre (1950). The *c* axis for $CaCO_3$, evident from the position of the 002 reflection, is smaller than for the borates, whereas the *a* axis (see 100 reflection) is larger. In the

TABLE 2. X-RAY DIFFRACTION DATA FOR ARAGONITE-TYPE ABO_3 BORATES (Cu $K_{\alpha 1}$ RADIATION)

hkl	$LaBO_3$[a] (1475°/ 1 hr.)		$LaBO_3$[b]		$NdBO_3$[c] (1075°/18 hr.)		$CaCO_3$[d]	
	*d*Å	RI%*	*d*Å	RI%*	*d*Å	RI%*	*d*Å	RI%*
110	4.34	12			4.27	21	4.21	2
020	4.12	4			4.04	10		
111	3.49	100	3.48	100	3.43	100	3.396	100
021	3.38	44	3.36	60	3.30	53	3.273	52
002	2.936	24	2.928	40	2.865	20	2.871	4
121	2.820	4			—	—	2.730	9
012	2.765	11			2.696	5	2.700	46
200	2.552	31	2.547	50	2.518	17	2.481	33
031	2.489	4			2.436	5	2.409	14
112	2.431	33			2.377	42	2.372	38
130	2.422	30	2.415	90	—	—	2.341	31
022	2.391	14	2.394	10	2.336	12	2.328	6
211	2.253	3			—	—	2.188	11
220	2.170	12	2.164	20	2.137	16	2.106	23
040	2.062	4			2.018	8		
221	2.036	47	2.034	100	2.003	50	1.977	65
041	1.947	17	1.940	50	1.903	22	1.882	32
202	1.926	27	1.919	50	1.893	23	1.877	25
132	1.868	37	1.863	90	1.828	34	1.814	33
141							1.759	4
113	1.784	21	1.778	90	1.744	25	1.742	25
231							1.728	15
023	1.769	17	1.762	10	1.727	14		
222	1.745	6	1.740	10	1.713	8	1.698	3
042	1.688	4			1.651	5		
310	1.667	3						
240 / 311	1.604	11	1.602	60	1.581	11	1.557	4
051/232							1.535	2
150			1.567	2				
241	1.548	11	1.545	50	1.519	11	1.499	4
321							1.475	3
151	1.517	15	1.513	60	1.484	10	1.466	5
223	1.454	8			1.425	15		
014/312			1.446	70			1.411	5

* RI is the intensity of each diffraction peak relative to the strongest peak.

[a] Orthorhombic cell: $a=5.104$, $b=8.252$, $c=5.872$ Å.

[b] Goldschmidt and Hauptmann, p. 67 (1931–32) *d* values calculated from corrected θ values listed by authors.

[c] Orthorhombic cell: $a=5.037$, $b=8.076$, $c=5.729$ Å.

[d] Swanson, Fuyat and Ugrinic (1954).

TABLE 2—(*continued*)

hkl	$LaBO_3$[a] (1475°/1 hr.)		$LaBO_3$[b]		$NdBO_3$[c] (1075°/18 hr.)		$CaCO_3$[d]	
	*d*Å	RI%*	*d*Å	RI%*	*d*Å	RI%*	*d*Å	RI%*
330	1.447	11					1.404	3
043	1.420	6						
242	1.408	4			1.381	5	1.365	3
114	1.391	8			1.358	5	1.358	3
060							1.328	2
332	1.298	15			1.276	9	1.261	6
400							1.240	7
204	1.272	8						
313	1.269	9			1.247	11		
134	1.255	19			1.227	7	1.224	5
062	1.246	6					1.205	6
243	1.2409	7						
153	1.2250	8					1.1892	5
260	1.2109	10					1.1712	6
421	1.1941	6					1.1599	3
402	1.1707	3						
351	1.1619	6						
115	1.1334	5						
025	1.1297	5						
262	1.1195	6						
314	1.1015	9						
244	1.0832	3						
441	1.0673	5						
423	1.0353	5						
225	1.0327	6						
334	1.0305	6						
045	1.0204	5						
442	1.0180	5						
353	1.0137	15						

vaterite-type borates, if the two weak reflections 101 and 103 were missing, the *c* axis would be halved. In $CaCO_3$, however, the 101 reflection is pronounced (see Fig. 4). Decreasing ionic radii of the rare earth ions from $SmBO_3$ to $LuBO_3$ are associated with decreasing interplanar spacings (larger two theta values) for corresponding reflections.

A number of the *x*-ray diffraction peaks, especially for angles larger than 60° 2θ, were broad and diffuse rather than narrow and sharp as is characteristic of well-crystallized material. Furthermore, the $K_{\alpha 1}$ and $K_{\alpha 2}$ doublets were not resolved in any of the vaterite patterns. Attempts to obtain better material by heating in the sealed platinum tubes for

periods of 64 hrs. at 1100° C. ($SmBO_3$, Table 1) and 23 hrs. at 1300° C. $ErBO_3$) were unsuccessful. Likewise, 5-minute heating periods in the induction furnace just above or below the melting points failed to produce sharper patterns. Study of $YbBO_3$ with a high-temperature x-ray spectrometer up to 1000° C. did not reveal any inversions or improvement of the pattern.

Optical examination showed that the vaterite-type borates had a moderately low birefringence, about .007 for $SmBO_3$ and $EuBO_3$, and

TABLE 3. X-RAY POWDER DIFFRACTION DATA FOR THE HIGH-TEMPERATURE FORM OF $LaBO_3$ (Cu $K_{\alpha 1}$ RADIATION)

Present Investigation (1580°/$\frac{5}{6}$ hr.)		Keith and Roy (1954) (below 1560°)	
dÅ	RI%*	dÅ	RI%*
6.03	10	5.64	7
3.98	20		
3.92	43	3.91	20
3.89	76		
3.13	44		
3.11	100	3.10	100
3.02	73	3.01	90
2.94	11		
2.87	11	2.86	5
2.60	13		
2.54	34	2.54	7
2.50	13		
2.143	26		
2.135	30	2.13	10
2.114	10	2.085	3
2.092	20	2.07	2
2.013	11	2.01	15
1.962	9		
1.948	28	1.946	5
1.919	56	1.916	15
1.902	21		
1.872	19	1.875	3
1.854	14		
1.831	26	1.828	7
1.738	9		
1.700	7		
1.631	10		
1.613	13	1.610	5
1.582	7		
1.556	10		

* RI is the intensity of each diffraction peak relative to the strongest peak.

TABLE 4. *X*-RAY DIFFRACTION DATA FOR $NdBO_3$, $SmBO_3$ AND $EuBO_3$ HIGH-TEMPERATURE POLYMORPHS ($CuK_{\alpha 1}$ RADIATION)

$NdBO_3$ (1475°/1 hr.)		$SmBO_3$ (1550°/1 hr.)		$EuBO_3$[a] (1575°/1 hr.)	
*d*Å	RI%[b]	*d*Å	RI%[b]	*d*Å	RI%[b]
6.17	16	6.07	13		
5.13	8	5.06	11		
4.29	52	4.26	56	4.26	48
3.65	58	3.60	72	3.60	58
3.61	49	3.56	28	3.55	35
3.20	8	3.15	13		
3.076	100	3.044	100	3.04	100
2.983	28	2.944	27		
2.968	33	2.926	29	2.91	42
2.839	26	2.832	20		
2.828	52	2.789	34	2.775	40
2.753	10	2.715	10		
2.577	18	2.556	30		
2.552	27	2.531	43		
2.507	6	2.490	9		
2.462	6				
2.391	13	2.356	15		
2.290	9	2.264	15		
2.177	20	2.158	26		
2.141	5	2.131	8		
2.100	10				
2.090	10	2.070	12		
2.051	9	2.026	20		
2.018	19				
2.000	19	1.997	23		
1.973	10				
1.957	7	1.953	21		
1.901	9	1.873	21		
1.861	10	1.837	20		
1.824	17	1.801	20		
1.801	13	1.779	21		
1.750	14				
1.735	14	1.728	24		
1.728	12	1.697	12		
1.719	8				
1.674	6				
1.654	11				
1.633	8	1.613	17		
1.603	8				

[a] Formed in quenched liquid, Vaterite is major phase present.

[b] RI is the intensity of each diffraction peak relative to the strongest peak.

TABLE 5. *X*-RAY POWDER DIFFRACTION DATA FOR VATERITE-TYPE ABO_3 RARE-EARTH BORATES ($CuK_{\alpha 1}$ RADIATION)

hkl[a]	$SmBO_3$ (1200°/24 hr.)		$EuBO_3$ (1450°/1 hr.)		$GdBO_3$ (1475°/1 hr.)		$DyBO_3$ (1475°/¾ hr.)		YBO_3 (1580°/1 hr.)		Keith & Roy (1954)	
	*d*Å	RI%[b]	*d*Å	RI%[b]	*d*Å	RI%[b]	*d*Å	RI%[b]	*d*Å	RI%[b]	*d*Å	RI%[b]
002	4.48	44	4.47	37	4.45	52	4.42	40	4.41	30	4.375	30
100	3.34	100	3.33	100	3.32	100	3.28	100	3.27	100	3.277	100
101	3.13	9	3.12	10	3.11	10	3.08	8	3.07	16	3.06	10
102	2.68	91	2.67	94	2.66	99	2.64	51	2.63	72	2.62	60
004	2.24	15	2.23	16	2.22	14	2.21	7	2.20	9		
103			2.22	7	2.20	6			2.19	4	2.195	10
110	1.930	48	1.922	46	1.915	42	1.896	25	1.888	87	1.885	35
104	1.861	41	1.856	40	1.848	49	1.834	17	1.826	59	1.82	25
112	1.773	41	1.766	34	1.760	23	1.742	13	1.735	54	1.73	20
200	1.672	19	1.665	16	1.658	13	1.641	9	1.636	10	1.631	7
202	1.566	26	1.561	21	1.554	21	1.539	9	1.533	13	1.532	15
006									1.468	2		
114	1.462	14	1.456	12	1.451	10	1.438	5	1.433	4		
106	1.363	14	1.359	12	1.354	15	1.344	3	1.338	6	1.337	5
204	1.340	13	1.334	14	1.330	15			1.313	6	1.311	2
210	1.263	13	1.258	12	1.253	12	1.242	5	1.236	5	1.328[c]	2
212	1.216	19	1.212	17	1.208	16	1.195	7	1.190	9	1.189	10
116			1.176	9					1.158	2		
008												
206												
300	1.113	10	1.110	11					1.090	4		
214	1.101	12	1.097	11					1.078	5		
302	1.080	8	1.076	9					1.058	3		
108									1.042	2		

hkl	$HoBO_3$ (1100°/19 hr.)		$ErBO_3$ (1550°/1 hr.)		$TmBO_3$ (1450°/1 hr.)		$YbBO_3$ (1551°/1 hr.)		$LuyBO_3$ (1450°/1 hr.)	
	*d*Å	RI%	*d*Å	RI%	*d*Å	RI%	*d*Å	RI%	*d*Å	RI%
002	4.41	61	4.38	32	4.38	43	4.37	34	4.35	54
100	3.27	100	3.25	100	3.25	100	3.23	100	3.23	100
101	3.06	11	3.05	11	3.04	6	3.03	7	3.02	5
102	2.63	89	2.62	76	2.61	74	2.60	71	2.59	78
004	2.20	15	2.20	8	2.19	10	2.18	8	2.18	15
103	2.19	4	2.18	2	2.17				2.16	2
110	1.888	32	1.880	40	1.873	35	1.866	37	1.861	35
104	1.827	35	1.821	28	1.816	27	1.811	25	1.805	32
112	1.735	24	1.729	28	1.723	26	1.717	27	1.713	27
200	1.635	8	1.629	13	1.622	11	1.616	14	1.613	12
202	1.533	12	1.527	17	1.522	14	1.516	16	1.513	14
006	1.465	2	1.462	2	1.461	1	1.456	1	1.453	2
114	1.432	6	1.429	7	1.423	6	1.419	7	1.419	7
106	1.340	7	1.335	6	1.331	6	1.328	5	1.325	7
204	1.313	6	1.309	7	1.304	6	1.300	6	1.298	7
210	1.236	4	1.231	7	1.227	6	1.222	7	1.219	6
212	1.190	8	1.186	11	1.181	9	1.177	10	1.174	9
116	1.160	2	1.155	3	1.153	3	1.149	2	1.146	2
008					1.096	1	1.092	1	1.089	2
206					1.087	3	1.083	3	1.082	3
300	1.090	4	1.086	5	1.082	4	1.078	4	1.076	4
214	1.078	4	1.074	6	1.071	5	1.067	5	1.065	5
302	1.058	3	1.055	4	1.050	4	1.046	4	1.044	3
108	1.043	2	1.041	2	1.038	2	1.035	2	1.032	2

[a] Unit cell dimensions for the hexagonal indices are listed in Table 9.

[b] RI is the intensity of each diffraction peak relative to the strongest peak.

[c] Out of order, possibly 1.238.

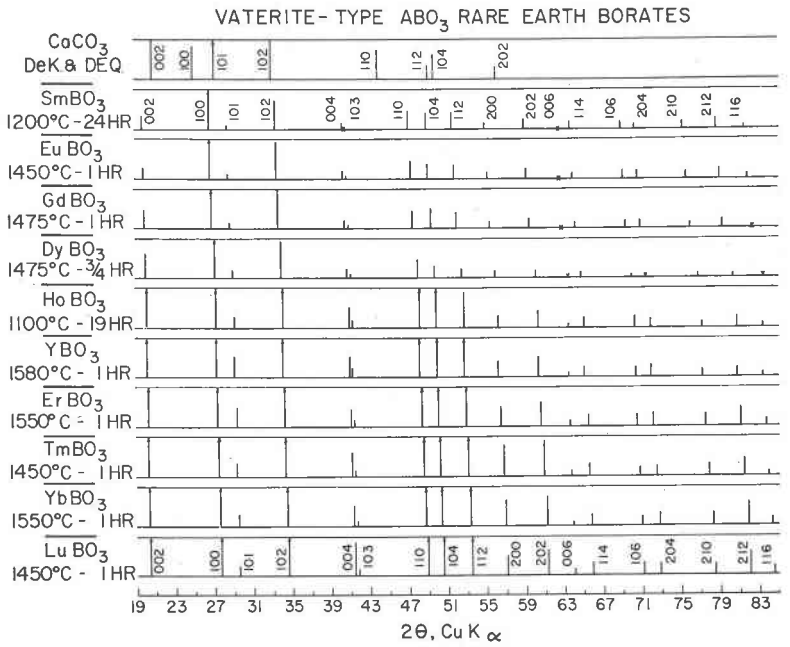

FIG. 4. Diagramatic *x*-ray diffraction patterns of the vaterite-type ABO_3 borates compared with $CaCO_3$. $CaCO_3$-vaterite after DeKeyser and Degueldre (1950).

about .015 for the others (Table 6). The indices of refraction decreased with decreasing radius of the rare earth cation from Sm^{+3} to Lu^{+3}. With the exception of Y^{+3} (not a rare earth), the indices are grouped by pairs, *e.g.*, $SmBO_3$ and $EuBO_3$, $GdBO_3$ and $DyBO_3$, etc. The positive character of the compounds was easily ascertained on off-centered interference figures. However, as the intersection of the isogyres was never observed, it was not possible to characterize the material as uniaxial, or biaxial with a small optic axial angle. No twinning phenomenon was apparent, although some of the sample showed good anhedral grain growth.

The most logical explanation for the *x*-ray and optical data is that vaterite-type borates are only pseudo-hexagonal.

An infrared examination made by C. Weir of this Laboratory showed that the pattern of μ-$CaCO_3$ was considerably different from that of the vaterite-type borates. In the three forms of $CaCO_3$, carbon is in a CO_3^{2-} planar group with three-fold oxygen coordination. However, the infrared patterns of the vaterite-type borates can be interpreted as indicating that boron has a tendency toward oxygen coordination greater than 3. A non-planar boron-oxygen configuration may explain the stability of the vaterite-type borates.

TABLE 6. OPTICAL PROPERTIES OF ABO_3 RARE-EARTH BORATES

Compound	Heat Treatment		Indices of Refraction (λ_D, 25° C.)			Sign	2V	Bire-fringence	Structure Type[b]
	Temp., °C.	Time, hrs.	alpha	beta	gamma				
Low-$LaBO_3$	1300	3¼	1.800	1.877	1.882	−	~20°	0.084	Aragonite
High-$LaBO_3$	1581	1	1.742	1.856	1.878	−	~50°	0.136	Unknown
Low-$NdBO_3$[a]	1075	18	..	..	..	..			Aragonite
High-$NdBO_3$	1475	1	1.789	..	1.883	−	medium	0.094	Unknown
High-$SmBO_3$	1550	1	1.789	..	1.897	−	medium	0.108	Unknown
			ordinary		extraordinary				
$SmBO_3$	1250	1	1.842		1.849	+[c]		0.007	Vaterite
$EuBO_3$	1525	1	1.841		1.848	+[c]		0.007	Vaterite
$GdBO_3$	1575[d]		1.824		1.840	+[c]		0.016	Vaterite
$DyBO_3$	1525[d]		1.823		1.837	+[c]		0.014	Vaterite
YBO_3	1645[d]		1.788		1.802	+[c]		0.014	Vaterite
$HoBO_3$	1475	1	1.816		1.830	+[c]		0.014	Vaterite
$ErBO_3$	1604[d]		1.815		1.830	+[c]		0.015	Vaterite
$TmBO_3$	1647[d]		1.812		1.828	+[c]		0.016	Vaterite
$YbBO_3$	1550	1	1.809		1.824	+[c]		0.015	Vaterite
High-$LuBO_3$	1647[d]		1.803		1.817	+[c]		0.014	Vaterite
Low-$LuBO_3$[a]	1297	17				−			Calcite
$InBO_3$	1475	1	1.873		1.773	−		0.100	Calcite

[a] Too fine grained to obtain optical data.
[b] From indexed x-ray powder pattern.
[c] From off-centered interference figure.
[d] Held at temperature in induction furnace for about 5 minutes.

The similarity of the x-ray data for vaterite-$CaCO_3$ and many of the borates indicates that the arrangements of the heavy cations are essentially the same. On the other hand, the dissimilarity of the infrared patterns indicates that some differences exist in the anion bonding configuration.

Yttrium Borate

It may be noted from Fig. 1 that YBO_3 lies in the middle of the field of vaterite-type compounds and that no polymorphism is indicated. Various contemporary texts on crystal chemistry list YBO_3 as having the calcite-type structure. The source of this statement is probably the original paper of Goldschmidt and Hauptmann (1931–32). They reported that a sample of YBO_3 quickly cooled from the melt gave a residue ("Reste") of the calcite-type structure. At lower temperatures, a "biaxial-crystal type" was found, which was believed to be related to the vaterite structure. It should be emphasized that the "yttrium" used by Goldschmidt and Hauptmann in the preparation of the yttrium borate was a mixture of yttrium earths of average atomic weight 104.7 (atomic wt. Y = 88.92), obtained from the mineral thalenite.

Keith and Roy (1954) found that only one crystalline form of YBO_3

existed from room temperature to the melting point. They concluded that their YBO_3 compound was not of the vaterite type when compared with the incomplete data of Brooks, Clark and Thurston (1951). However, the *x*-ray data of Keith and Roy and that obtained in the present study are in good agreement (Table 5). The melting point of YBO_3 ($1650 \pm 20°$ C.) determined by the inductively heated iridium crucible method is some 70° C. above that reported by Keith and Roy ($1580 \pm 20°$ C.) using a strip furnace.

Calcite-Type ABO_3 Borates

Lutecium borate, formed from the smallest rare-earth ion, and indium borate were the only two calcite-type structures found in this study. Lutecium borate showed a reversible transformation at 1310° C. from the low-temperature calcite form to the high-temperature vaterite form.

The *x*-ray diffraction data for the calcite-type borates are given in Table 7, together with the data of Goldschmidt and Hauptmann for $InBO_3$. For purposes of comparison the data for calcite are given, and both rhombohedral and hexagonal indexing are shown. A diagrammatic comparison of the powder patterns is shown in Fig. 5. The space group for calcite is $R\,\bar{3}c$, with 6 molecules per unit cell when indexed on a hexagonal basis.

In $InBO_3$, the *c* axis (from the 006 reflection) is considerably less than in $LuBO_3$, but the *a* axis (from the 110 reflection) is only slightly smaller. Consequently, for large values of *l* relative to *hk*, a number of reversals occur in the order of the position of the reflections, *e.g.*, 108/116 and

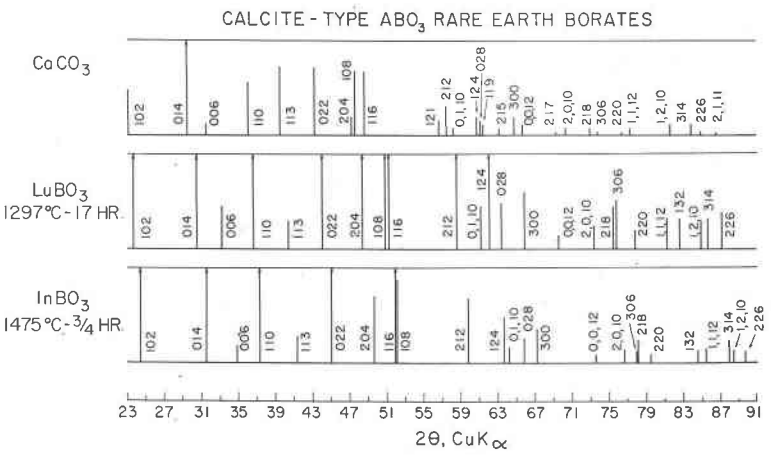

FIG. 5. Diagrammatic *x*-ray diffraction patterns of the calcite-type ABO_3 borates compared with $CaCO_3$. $CaCO_3$-calcite after Swanson and Fuyat (1953).

TABLE 7. *X*-RAY POWDER DIFFRACTION DATA FOR CALCITE-TYPE ABO_3 BORATES ($CuK_{\alpha 1}$ RADIATION)

Rhombo-hedral	Hexag-onal	$CaCO_3$[a]		$LuBO_3$		$InBO_3$		$InBO_3$ Gold. & Haupt. (1931–32)	
hkl	*hkl*	*d*Å	RI%[b]	*d*Å	RI%[b]	*d*Å	RI%[b]	*d*Å[c]	RI%[b]
110	102	3.86	12	3.76	96	3.67	100	3.68	50
121	014	3.035	100	2.933	100	2.836	98	2.840	60
222	006	2.845	3	2.699	10	2.574	5	2.583	5
011	110	2.495	14	2.453	53	2.411	36	2.414	40
120	113	2.285	18	2.235	7	2.184	7	2.193	20
020	022	2.095	18	2.057	44	2.016	28	2.016	40
220	204	1.927	5	1.883	26	1.837	20	1.837	30
332	108	1.913	17	1.828	31	1.753*	21	1.756	100
231	116	1.875	17	1.817	54	1.760	36		
$02\bar{1}$	121	1.626	4						
$12\bar{1}$	212	1.604	8	1.577	27	1.547	19	1.546	60
343	0·1·10	1.587	2	1.515	10	1.450*	5	1.457	60
130	124	1.525	5	1.495	23	1.462	14		
242	028	1.518	4	1.468	11	1.418	8	1.418	30
342	119	1.510	3						
230	215	1.473	2						
$11\bar{2}/\bar{1}2\bar{1}$	300	1.440	5	1.418	14	1.392	10	1.390	50
444	0·0·12	1.422	3	1.351	4	1.288	2	1.287	20
241	127	1.356	1						
442	2·0·10	1.339	2	1.290	6	1.242	4	1.243	20
341	218	1.297	2	1.260	10	1.222*	7	1.222	80
141/330	306	1.284	1	1.256	12	1.225	4		
$02\bar{2}$	220	1.247	1	1.228	5	1.206	3	1.206	20
453	1·1·12	1.235	2	1.184	8	1.136*	4	1.136*	40
$03\bar{1}$	132	—	—	1.168	7	1.146	4	1.145	40
352	1·2·10	1.180	3	1.142	7	1.104*	4	1.105	60
$23\bar{1}$	314	1.154	3	1.133	8	1.110	6		
240	226	1.1425	1	1.118	8	1.092	4	1.091	50
452	2·1·11	1.1244	<1					1.0357	10
464	0·2·14	1.0613	1			0.9761*	1	0.9760*	20
554	1·0·14					1.0673	1	1.0681	20
$22\bar{2}$	402			1.0547	2				
040	044	1.0613	1	1.0290	4	1.0081	3	1.0068	30
251	138	1.0447	4	1.0199	7	.9935	4	.9924	50
$13\bar{2}$	322					.9511	3	.9498	50

* Reversal in order of *hkl* $CaCO_3$-calcite.

[a] Swanson and Fuyat (1953).

[b] RI is the intensity of each peak relative to the strongest peak.

[c] Converted from corrected 2θ to interplanar spacing.

TABLE 7—(*continued*)

Rhombo-hedral	Hexag-onal	$CaCO_3$[a]		$LuBO_3$		$InBO_3$		$InBO_3$ Gold. & Haupt. (1931–32)	
hkl	*hkl*	*d*Å	RI%[b]	*d*Å	RI%[b]	*d*Å	RI%[b]	*d*Å[c]	RI%[b]
363/552	0·3·12					.9455	4	.9445	60
565	0·1·16					.9412	2		
$14\bar{1}$	234					.9304	3		
451	3·1·10					.9268	2	.9278	60
440	408					.9188	2	.9179	20
$12\bar{3}/13\bar{2}$	410					.9117	2	.9112	40
563	2·1·14					.9048	2	.9041	20
462	2·2·12					.8803	2	.8800	50
664	2·0·16					—	—	.8781	20
—	—					—	—	.8660	10
$150/34\bar{1}$	146					.8595	4	.8579	100
666	0·0·18					.8587	3		
						.8307	1		
						.8240	2		
						.8144	3		
						.8088	2		
						.8039	2		
						.7993	1		
						.7853	2		

0, 1, 10/124 pairs. No reversals in line position occur for the portion of the patterns of $CaCO_3$ and $LuBO_3$ that are shown in Fig. 5.

Scandium borate, reported by Goldschmidt and Hauptmann (1931–32) as having the calcite structure, was not investigated. As Mn_2O_3 has the same structure as Sc_2O_3 a composition of one to one molar ratio of Mn_2O_3 to B_2O_3 was investigated for compound formation. No calcite-type compound was formed (Table 1).

Birefringence of $InBO_3$ was found to be 0.100 (Table 7). According to Hartshorne and Stuart (1952, pg. 148), the greater the oxygen-oxygen separation in a planar group the less the birefringence, because of less inductive effect between the oxygens. The oxygen-oxygen separation in a BO_3^{3-} group was calculated to be about 2.38 Å, from data on $Co_3(BO_3)_2$ and $Mg_3(BO_3)_2$ structures given in Tables of Inter-atomic Distances (1958). This separation is larger than that in the CO_3^{2-} group (2.18 Å) and the NO_3^-group (2.10 Å). Consistent with the principle stated above, with decreasing oxygen separation, the birefringence of the calcite structures increases from 0.100 for $InBO_3$ to 0.172 for $CaCO_3$ to 0.250 for $NaNO_3$.

Factors Affecting Polymorphism

The unit cell parameters for the indexed ABO_3 polymorphs obtained in this study are given in Table 8, together with the larger cation radii, radius ratios (A^{3+}/O^{2-}) and the densities calculated from the *x*-ray powder patterns. Cation radii in parentheses are taken from Roth and Schneider (1960), as determined from a plot of the unit cell dimensions of the C-type rare-earth oxide structures versus the cation radius.

A comparison of the radius ratios for the ABO_3 compounds of the carbonates, borates, and nitrates is instructive. In the carbonates a radius ratio of 0.71 (Ca^{2+}/O^{2-}) appears to be critical. Compounds with radius ratios above 0.71, *e.g.*, $SrCO_3$ and $BaCO_3$, form an aragonite type

TABLE 8. UNIT CELL DIMENSIONS OF ABO_3 RARE-EARTH BORATES

Compound	[a]Radius of A^{3+} Å	[b]Radius ratio	*a*Å	*b*Å	*c*Å	Hex. c/a	[c]Density, Calc. g/cc
Aragonite-Type							
$LaBO_3$	1.14	0.81	5.104	8.252	5.872		5.309
$NdBO_3$	1.04	0.74	5.037	8.076	5.729		5.786
$CaCO_3$	0.99	0.71	4.959	7.968	5.741		2.930
Vaterite-Type							
$CaCO_3$	0.99	0.71	4.134		8.47	2.05	2.65
$SmBO_3$	1.00	0.71	3.858		8.96	2.32	6.01
$EuBO_3$	0.98	0.70	3.845		8.94	2.32	6.12
$GdBO_3$	0.97	0.69	3.829		8.89	2.32	6.36
$DyBO_3$	0.92	0.66	3.791		8.84	2.33	6.68
YBO_3	0.92 (.91)	0.66 0.65	3.777		8.81	2.33	4.51
$HoBO_3$	0.91	0.65	3.776		8.80	2.33	6.84
$ErBO_3$	0.89	0.64	3.761		8.79	2.34	6.97
$TmBO_3$	0.87	0.62	3.748		8.76	2.34	7.13
$YbBO_3$	0.86	0.614	3.732		8.74	2.34	7.30
$LuBO_3$	0.85	0.607	3.725		8.71	2.34	7.42
Calcite-Type							
$CaCO_3$[d]	0.99	0.71	4.989		17.062	3.420	2.711
$LuBO_3$[e]	0.85	0.61	4.913		16.214	3.300	6.871
$InBO_3$[f]	0.81 (.77)	0.58 0.55	4.823		15.456	3.204	5.555

[a] Ahren's radii. Values in parenthesis after Roth and Schneider (1960).
[b] Ratio of radii of rare earth cation to oxygen ion.
[c] From lattice parameters, with Z=4 for aragonite, 2 for vaterite, and 6 for calcite.
[d] For rhombohedral cell: $a=6.375$ Å, $\alpha=46.08°$.
[e] For rhombohedral cell: $a=6.104$ Å, $\alpha=47.46°$.
[f] For rhombohedral cell: $a=5.856$ Å, $\alpha=48.64°$.

structure at room temperature and calcite type structure at elevated temperatures. Below a radius ratio of 0.71, *e.g.*, $CdCO_3$, $ZnCO_3$, and $MgCO_3$, calcite-type structures are found. Calcium carbonate at room temperature shows both aragonite and calcite, with the exact stability relationships somewhat in question. This carbonate is the only one which can form a vaterite phase.

The stability relationships of the borate polymorphs are different. Above a radius ratio of 0.71, the aragonite-type borates are stable at room temperature, *e.g.* $NdBO_3$ and $LaBO_3$. Between radius ratios of 0.71 (for $SmBO_3$) and 0.61_4 (for $YbBO_3$), the vaterite-type exists as the only stable phase. At radius ratio 0.60_7 (for $LuBO_3$), the vaterite-type structure is stable above 1310° C.; the calcite-type structure is stable below this temperature. Below a radius ratio of 0.60_7 the calcite-type structure is stable, *e.g.*, $InBO_3$ and $ScBO_3$.

It is interesting to note that $CdCO_3$ among the carbonates and $NaNO_3$ among the nitrates with radius ratios of 0.69 and 0.67, respectively, form calcite-type structures even though the radius ratios fall within the vaterite group when compared with the borates. However, the radius ratio for $NaNO_3$ is 0.54 when based on univalent cation and anion values (Na^+/O^-) (Pauling, 1960). This radius ratio would place it in the calcite group, as the 0.61 borate tolerance ratio would not be greatly lowered when calculated for univalent radii. The next larger alkali ion, K^+, forms aragonite-type KNO_3; thus it is not surprising that a stable vaterite-type structure is not found in the nitrates.

Another significant comparison between the borates and carbonates concerns the densities of the vaterite and calcite-type structures. Whereas the vaterite form of $CaCO_3$ has a slightly lower density than the calcite form at atmospheric pressure, $LuBO_3$-vaterite type has a considerably higher density than the calcite-type polymorph (Table 8). The vaterite-type structure still would be more dense than the calcite-type structure at the temperature of transition, 1310° C., because of the large difference in room-temperature densities of about 0.55 g/cc. Jamieson (1957) did not find a change in x-ray pattern when precipitated $CaCO_3$-vaterite containing 10% calcite was pressure cycled up to a maximum of 24,000 bars. Applying LeChatelier's Theorem to the transition of $LuBO_3$ from the low-temperature-calcite type to the high-temperature, denser vaterite form, the effect of increased pressure would be to lower the transition temperature, or at constant temperature to favor the transition.

An increase in pressure would not favor the formation of a calcite-type structure for any of the rare earth borates. Unit cell dimensions and densities of calcite-type structures can be postulated for the rare earth borates, by extrapolation of data from known calcite-type borates. The

postulated calcite-type structures would always be the least dense, as in the case of $LuBO_3$. The fact that the vaterite-type borate has a greater density than the calcite type is consistent with the postulated nonplanar configuration of the BO_3^{3-} group in the vaterite-type structure, which would result in more efficient packing.

Lander (1949) reported that $BaCO_3$ and $SrCO_3$, which have the aragonite structure at room temperature, show a calcite-type structure at elevated temperatures. The calcite-type structure was not quenchable but was observed with high-temperature *x*-ray equipment. The possibility should be considered that $LaBO_3$ and $NdBO_3$, for example, might possess a non-quenchable calcite-type polymorph. High-temperature *x*-ray diffraction patterns showed only the aragonite-type structure up to 1100° C. Therefore, such a transformation seems unlikely.

A consideration of the reported tentative crystal structure of $CaCO_3$-vaterite together with the infrared data of the vaterite-type borates is instructive. Both Hans-Jurgen Meyer (1959) and McConnell (1960) independently arrived at the conclusion that $CaCO_3$-vaterite is one end member of the group bastnaesite ($CeFCO_3$)-parisite ($2CeFCO_3 \cdot CaCO_3$)-roentgenite ($3CeFCO_3 \cdot 2CaCO_3$)-synchisite ($CeFCO_3 \cdot CaCO_3$)-vaterite ($CaCO_3$). However, Donnay and Donnay (1953) conclude that "compositions richer in calcium than synchisite with analogous crystal structures are not to be expected," because with the nearly vertical arrangement of the carbonate groups, the calcium coordination number would be too low. In accordance with this conclusion, $CaCO_3$-vaterite only exists metastably. However, as mentioned previously, the infrared data for the vaterite-type borates indicate that the anion configuration is different from that in $CaCO_3$-vaterite. This difference may account for the greater stability of the vaterite borates.

Summary

(1) Polymorphic relationships as a function of temperature and ionic radius were investigated for thirteen ABO_3-type borates, including all of the normally trivalent rare earth ions as well as La^{+3}, Y^{+3}, In^{+3}, and Mn^{+3}. The chief method of identification was by means of *x*-ray powder diffraction techniques.

(2) The melting points of the ABO_3 compounds determined with an inductively heated iridium crucible were found to be within $\pm 20°$ C. as follows: $LaBO_3$-1660° C.; $NdBO_3$-1570° C.; $SmBO_3$-1545° C.; $EuBO_3$-1540° C.; $GdBO_3$-1590° C.; $DyBO_3$-1585° C.; YBO_3-1650° C.; $HoBO_3$-1605° C.; $ErBO_3$-1630° C.; $TmBO_3$-1650° C.; $YbBO_3$-1590° C.; $LuBO_3$-1650 C., and $InBO_3$-1610° C.

(3) In general, the borate compounds had the same structure types as

the three forms of $CaCO_3$, *i.e.*, aragonite, vaterite, and calcite.

(4) $LaBO_3$ and $NdBO_3$ showed a low-temperature aragonite-type structure. At 1488° C. and 1090° C., respectively, they transformed to high-temperature forms, which were different from each other.

(5) Above 1285° C., $SmBO_3$ showed the same high-temperature polymorph as $NdBO_3$. The stable polymorph below this temperature was vaterite. The behavior of $SmBO_3$ was interesting in that the high form occurred metastably below about 1050° C.

(6) Whereas vaterite only forms metastably in the $CaCO_3$ system, the following borates were found to have a stable vaterite-type phase up to the melting point: $EuBO_3$, $GdBO_3$, $DyBO_3$, YBO_3, $HoBO_3$, $ErBO_3$, $TmBO_3$, and $YbBO_3$.

(7) Lutecium borate, containing the smallest rare earth ion, was found to have a reversible transformation at 1310° C. between the vaterite-type structure at high temperature and the calcite-type structure at low temperature. Indium borate existed only as the calcite form. Yttrium borate did not form a calcite-type structure, as often reported in the literature. Preliminary experiments to form a $MnBO_3$ carbonate-type structure were unsuccessful.

(8) Optical and x-ray examination of the ABO_3 vaterite-type compounds indicated that the unit cell might be only pseudo-hexagonal.

(9) A discussion of radius ratio, density, and pressure, in addition to interpretation of infrared and structure data may explain why the vaterite-type structure is more stable in the borates than in the carbonates.

(10) A comparison of the published powder diffraction data for vaterite is given in an appendix.

References

Brooks, R., Clark, L. M. and Thurston, E. F. (1950–51), Calcium carbonate and its hydrates: *Phil. Trans. Royal Soc.*, **243A,** 145–167.

DeKeyser, W. L. and Degueldre, L. (1950), Contribution à l'étude de la formation de la calcite, aragonite et vatérite: *Bull. Soc. Chim. Belg.* **59,** 40–71.

Donnay, G. and Donnay, J. D. H. (1953), The crystallography of bastnaesite, parisite, roentgenite, and synchisite: *Am. Mineral.*, **38,** 932–963.

Gibson, R. E., Wyckoff, R. W. G. and Merwin, H. (1925), Vaterite and μ-calcium carbonate: *Am. J. Sci.*, **10**/5th series/325–333.

Goldschmidt, V. M. and Hauptmann, H. (1931–32), Isomorphie von Boraten und Karbonaten: *Nachr. Ges. Wiss. Gott. Math-Phys. Kl.*, 53–72.

Hartshorne, N. H. and Stuart, A. (1952), Crystals and the Polarising Microscope: Edward Arnold & Co., London.

Heide, F. (1924), Vaterite: *Centralblatt für Mineralogie, Geologie, und Paläontologie,* **21,** 641–651.

Jamieson, J. C. (1957), Introductory studies of high-pressure polymorphism to 24,000 bars by x-ray diffraction with some comments on calcite II: *J. Geol.*, **65,** 334–343.

Keith, M. L. and Roy, R. (1954), Structural relations among double oxides of trivalent elements: *Am. Mineral.*, **39,** 1–23.

LANDER, J. J. (1949), Polymorphism and anion rotational disorder in the alkaline earth carbonates: *J. Chem. Physics*, **17,** 892–901.

LEVIN, E. M., ROBBINS, C. R. AND WARING, J. L. (1961), Immiscibility and the system lanthanum oxide-boric oxide: *Jour. Am. Cer. Soc.*, **44,** 87–91.

MCCONNELL, J. D. C. (1960), Vaterite (μ-$CaCO_3$) from Ballycraigy, Larne, Northern Ireland; Exhibit: *Min. Mag.*, **32,** [249], lxvii. Publication: *Min. Mag.*, **32,** [250], 535–544 (1960).

MEIGEN, E. W. G. (1911), *Verh. Ges. deutsch. Naturfor., Ärzte Königsberg*, **2,** 124.

MEYER, HANS-JURGEN (1959), Über Vaterit und seine Struktur: *Angewandte Chemie, Dtsch.* **71** [21], 678–9.

OLHAUSEN, S. (1925), Strukturuntersuchungen nach die Debye-Scherrer Methode: *Zeit. Krist.*, **61,** 463–514.

PAULING, L. (1960), The Nature of the Chemical Bond: Cornell Univ. Press, Ithaca, N. Y.

PHEMISTER, D. B., ARONSOHN, H. G. AND PEPINSKY, R. (1939), Variations in the cholesterol bile pigment and calcium salts contents of gallstones formed in gall-bladder and in bile ducts with the degree of associated obstruction: *Ann. Surg.*, **109,** 161–186.

PRIEN, E. L. AND FRONDEL, C. (1947), Studies in urolithiasis: I. The composition of urinary calculi: *J. Urology*, **57**/6/949–991.

RINNE, F. (1924), III. Rontgenographische Untersuchungen an feinzerteilten Mineralien, Kunstprodukten und dichten Gesteinen: *Zeit. Krist.*, **60,** 55–69.

ROTH, R. S. AND SCHNEIDER, S. J. (1960), Phase equilibria in systems involving the rare earth oxides: Part I. Polymorphism of the oxides of the trivalent rare earth ions: *J. Research Nat. Bur. Standards*, **64A,** 309–316.

SCHNEIDER, S. J. (1961), *ibid.* Part III. The Eu_2O_3-In_2O_3 System: *J. Research Nat. Bur. Standards*, **65A,** 429–434.

SCHNEIDER, S. J. AND ROTH, R. S. (1960), *ibid.* Part II. Solid State Reactions in Trivalent Rare-Earth Oxide Systems: *J. Research Nat. Bur. Standards*, **64A,** 316–332.

SWANSON, H. E. AND FUYAT, R. K. (1953), Standard *x*-ray diffraction powder patterns: *Nat. Bur. Standards Circular 539*, Vol. **II,** 52.

SWANSON, H. E., FUYAT, R. K., AND UGRINIC, G. M. (1954), Standard *x*-ray diffraction powder patterns: *Nat. Bur. Standards Circular 539, Vol.* **III,** 54.

TABLES OF INTERATOMIC DISTANCES AND CONFIGURATION IN MOLECULES AND IONS (1958), The Chemical Society, Burlington House, London.

WYCKOFF, R. W. G. (1931), The Structure of Crystals, 2nd ed.: The Chemical Catalog Co., Inc., New York.

X-RAY POWDER DATA FILE (1959), Published by American Soc. for Testing Materials, Phila. 3, Pa.

Manuscript received November 8, 1960.

APPENDIX

Vaterite-Type $CaCO_3$

The literature pertaining to the *x*-ray data for vaterite is widely scattered and has never been summarized. All published *x*-ray data have been obtained from poorly crystalline artificial preparations. Although vaterite has been recognized as a constituent of gall stones (Phemister, *et al.*, 1939), it has only recently been found as a naturally occurring mineral (McConnell, 1960).

Early confusion in the naming and identification of vaterite was clarified by Gibson, Wyckoff, and Merwin (1925), who were among the first to apply *x*-ray powder diffraction techniques to the problem. They stated that the name vaterite was first used by Meigen (1911) as an abbreviation for "Vater's Third Modification of Calcium Carbonate."

TABLE 9. REPORTED *X*-RAY POWDER DIFFRACTION DATA FOR $CaCO_3$-VATERITE

hkl	Rinne (1924)		Heide[a] (1924)		Olhausen[b] (1925)		Gibson *et al.* (1925)		Prien & Frondel[c] (1947)		ASTM[d]		DeKeyser & Degueldre[e,f] (1950)	Brooks *et al.*,[f] (1950–51)	McConnell[g] (1960)		Present Work	
	*d*kx	I[h]	*d*kx	I[h]	*d*kx	I[h]	*d*kx	I[h]	*d*kx	RI%[i]	*d*Å	RI%[i]	*d*Å	*d*kx	*d*Å	I[h]	*d*Å	RI%[i]
002			4.30	s	4.29	s					4.26	13	4.278		4.26	m	4.25	25
100	3.5	w	3.59	m	3.58	m	3.59	s	3.59	70	3.58	63	3.568	3.56	3.58	s	3.586	66
101	3.3	m+	3.29	m	3.28	m	3.29	s	3.29	70	3.29	75	3.282	3.278	3.30	s	3.302	100
102	2.7	s+	2.73	s	2.72	s	2.719	s−	2.72	60	2.73	100	2.714	2.714	2.73	s	2.737	89
			2.55	vw	2.55(?)	vw												
j			2.31	m	2.30	m	2.313	vw	2.31	10	2.31	8			2.33} 2.30}	wb	2.312	8
															2.23	w	2.221	7
103															2.127	w	2.119	11
004															2.059	s	2.067	49
110	2.1	s+	2.08	s	2.07	s	2.058	s+	2.06	100	2.06	63	2.06		1.856	w	1.856	21
112							1.85	w	1.85	20	1.87	15	1.856		1.825	s	1.823	43
104	1.8	s+	1.85	s	1.84	s	1.82	w	1.82	20	1.83	63	1.835				1.792	6
200																		
202	1.6	s	1.65	m	1.65	m	1.64	m	1.64	40	1.65	31	1.641	1.635	1.648	wb	1.648	17
105[k]			1.55	w	1.55	w	1.537	w	1.54	20	1.55	8			1.544	vw	1.544	3
114	1.5	w					1.467	vw	1.47	10	1.48	8			1.480	vw	1.479	5
															1.416	vw		
204			1.37	w	1.37	w	1.364	vw	1.36	10	1.37	8			1.369	vw	1.368	5
106			1.31	w	1.31	w					1.32	10			1.316	w	1.312	7
212	1.3	m+	1.29	w	1.28	w	1.283	m	1.28	40	1.29	13			1.288	vw	1.287	8
															1.185	vw		
															1.166	w		
302/214[k]			1.14	vw	1.14	vw	1.14	vw	1.14	10	1.15	8			1.141	w	1.143	6
206			1.11	vw	1.11	vw	1.105	vw	1.11	10	1.11	5			1.112	w	1.107	4
			1.02	vw	1.02	vw												
			0.979	vw	0.977	vw												
			0.946	vw	0.944	vw												

[a] *d* values calculated by present authors from film distances, assuming a 40 mm camera radius.
[b] No radiation wavelength data given. *d* values calculated by present authors from $\theta/2$ observed. Gives *hkl* values.
[c] Also *X*-ray Powder Data File, Card #4-0844.
[d] *X*-ray Powder Data File, Card #1-1032, $a=4.120$ Å, $c=8.556$ Å, $c/a=2.073$.
[e] Gives *hkl* values. $a=4.120$ Å, $c=8.556$ Å.
[f] No intensities given.
[g] Pattern originally indexed on unit cell relationship: $a'=a\sqrt{3}$, $c'=c$. Thirteen additional *d* values not listed here.
[h] s—strong, m—medium, w—weak, vw—very weak, b—broad.
[i] RI is the intensity of each diffraction peak relative to the strongest peak.
[j] The corresponding *d* value cannot be indexed on the basis of the hexagonal cell but is believed to be part of the vaterite diffraction pattern.
[k] These *hkl* values do not give a satisfactory fit with either hexagonal cell.

Table 9 lists the *x*-ray powder diffraction data for vaterite as reported by different investigators. Rinne (1924) and Heide (1924) were the first to report *x*-ray data. Heide, unfortunately, did not list *d* values, but they were calculated by the present authors from his stated film distances by assuming a 40 mm. camera radius.

Olhausen (1925) continued Heide's study of vaterite. He did not report radiation wavelength data or *d* values. The latter were calculated by the present authors, by conversion of his '$\theta/2$ observed' data. Olhausen was the first to show that vaterite crystallizes in the hexagonal system. He indexed the powder pattern on essentially the same unit cell as that used by later investigators: $a=4.110$ kX, $c=8.513$ kX, with 2 molecules per unit cell. However, his reported c/a ratio, 1.036, is exactly half of that calculated from his stated unit cell dimensions. An additional complication arises from the fact that Olhausen used a left-handed coordinate system. For interplanar spacings in the hexagonal system, he used the formula: $Q=p(h_1^2+h_2^2-h_1h_2)+qh_3^2$, which is equivalent, in conventional terminology, to:

$$\frac{1}{d^2}=\frac{h^2+k^2-hk}{a^2}+\frac{l^2}{c^2}.$$

The accepted formula for interplanar spacing, however, is:

$$\frac{1}{d^2}=\frac{h^2+k^2+hk}{a^2}+\frac{l^2}{c^2}.$$

Therefore, in order to convert Olhausen's indices, the value of the expression h^2+k^2-hk, using his indices, must be made equivalent to the sum of h^2+k^2+hk, from which the equivalent indices can be deduced.

Gibson, Wyckoff, and Merwin (1925), pg. 961, showed that the calcium carbonate of spherulitic habit investigated by Rinne, Heide, and several others, was essentially Vater's μ-calcium carbonate (true vaterite); whereas, the form originally designated 'vaterite' was in reality calcite. Gibson, *et al.* and Olhausen apparently were unaware of each other's work. The data of Prien and Frondel (1947), also listed in the *X*-ray Powder Data File (Card No. 5-0844), is probably that of Gibson, *et al.*, with *d* values rounded off to 3 figures and intensities given as percentages.

The *X*-ray Powder Data File contains a second vaterite pattern (Card No. 1-1032), the original source of which is not given. Although indexing is absent, the unit cell dimensions are listed as $a=4.120$ Å, $c=8.556$ Å, apparently obtained from Wyckoff (1931, p. 273).

DeKeyser and Degueldre (1950) and Brooks, Clark and Thurston (1950–51) have reported some of the major interplanar spacings for vaterite found in their studies of the factors governing the formation of calcium carbonate phases from solution. DeKeyser and Degueldre indexed their pattern using the same unit cell dimensions listed by Wykcoff (1931).

The crystal structure of vaterite was reported by Hans-Jurgen Meyer (1959) as a variant of the NiAs-type in which the plane of the CO_3-group is parallel to the *c* axis. He stated that vaterite was probably only pseudo-hexagonal, orthorhombic space group Pbnm, $a=4.13$ Å, $b=a\sqrt{3}$, $c=8.48$ Å, $Z=4$. These unit cell dimensions correspond closely to those found in the present work for a specimen of pure vaterite supplied by D. Graf of the Illinois Geological Survey: $a=4.134$ Å, $c=8.47$ Å. McConnell (1960), however, reported $c=8.524$ Å, which value is in closer agreement to that reported by Olhausen (1925). The differences in *c* dimensions might be related to the methods for precipitation of vaterite.

McConnell (1960) also concluded that the true unit cell of vaterite is hexagonal with *a* equal to $\sqrt{3}$ times the *a* value reported by previous investigators. On the basis of the larger cell an attempt was made to index the *x*-ray diffraction data for the vaterite used in the present study (Table 9). Three interplanar spacings, namely, 2.312 Å, 1.544 Å, and 1.143 Å,

however, could not be satisfactorily indexed on the basis of either cell. These discrepancies lend support to the conclusion made for the vaterite-type borates that the symmetry of vaterite is only pseudohexagonal.

Note Added in Press

Since acceptance of this paper for publication, differential thermal analysis and high-temperature *x*-ray data have shown that the vaterite-type rare-earth borates have an unquenchable high-temperature polymorph. The *x*-ray diffraction pattern of the high-temperature form is characterized by a c/a ratio very close to that of $CaCO_3$-vaterite, and the appearance of a new peak indexable as the (200) on the basis of a unit cell with $a=\sqrt{3}\,a'$ and $Z=6$. It must be concluded that the high-temperature form is most nearly isostructural with $CaCO_3$-vaterite, whereas the low-temperature form has a slightly different structure of greater density. The high-temperature *x*-ray patterns never showed improved crystallinity, thus still indicating that both forms are not truly hexagonal. The transition temperatures on heating and cooling, respectively, were found by DTA to be as follows: $SmBO_3$—834°, 530° C.; $EuBO_3$—878°, 561° C.; $GdBO_3$—927°, 578° C.; $DyBO_3$—999°, 627° C.; YBO_3—1024°, 600° C.; $HoBO_3$—1020°, 646° C.; $ErBO_3$—1022°, 632° C.; $TmBO_3$—1040°, 604° C.; $YbBO_3$—1041°, 577° C.; and $LuBO_3$ (metastable inversion)—1037°, 538° C. High-temperature *x*-ray data for $YbBO_3$ at 1050° C. are as follows: low form—$a=6.542$A, $c=8.771$A, $c/a=1.341$, $\rho=7.104$ g/cm^3; high form—$a=6.987$A, $c=8.336$A, $c/a=1.193$, $\rho=6.552$ g/cm^3. Even though previous thermal history may affect the high↔low vaterite inversion, the very large hysteresis has been found to be relatively independent of the heating rate. For example, no transformation was observed in $SmBO_3$ after holding, in the high-temperature *x*-ray furnace, either the low-vaterite form at 800° C. for 22 hours or the high-vaterite form at 600° C. for 66 hours.